Resources, Conservation & Recycling 210 (2024) 107826

Contents lists available at ScienceDirect

Resources, Conservation & Recycling

journal homepage: www.sciencedirect.com/journal/resources-conservation-and-recycling

Mechanism and performance of the hydrolytic chemical recycling of polylactide catalyzed by the protic ionic liquid 2-HEAA

A. Cháfer [a], O. Gil-Castell [a], A. Björling [b], R. Ballesteros-Garrido [c], J.P. Cerisuelo-Ferriols [a], J. D. Badia [a,*]

[a] Research Group in Materials Technology and Sustainability (MATS), Department of Chemical Engineering, School of Engineering, Universitat de València, Av. Universitat s/n, 46100 Burjassot, Valencia, Spain
[b] Polymer and Fibre Technology, Kungliga Tekniska Högskolan, Teknikringen 56-58, 100 44 Stockholm, Sweden
[c] Department of Organic Chemistry, Universitat de València, C/ Dr Moliner 50 Burjassot, 46100, Valencia, Spain

ARTICLE INFO

Keywords:
Chemical valorization
Hydrolysis
Polylactide (PLA)
Protic ionic liquid (PIL)
2-hydroxyethyl ammonium acetate (2-HEAA)
Mechanisms
Kinetics

ABSTRACT

The hydrolytic chemical recycling of polylactide (PLA) aided by the protic ionic liquid 2-hydroxyethyl ammonium acetate (2-HEAA) as a homogeneous catalytic co-solvent was evaluated. In terms of maximization, temperature emerged as the most significant factor, being milder compared to that applied with other catalysts, resulting in potential energy savings. From a cost-efficiency perspective, employing a high solvent proportion was deemed unnecessary, thereby reducing reagent consumption. A higher proportion of ionic liquid leads to higher conversions, which could be trace-free recovered and reused in subsequent recycling steps. The best reaction triplet was a temperature of 140 °C, a mass ratio between PLA and water of 1:6, and a mass ratio between PLA and 2-HEAA of 1:2.5, enhancing the efficiency of PLA conversion under a waste-to-gate circular model in the chemical valorization industry. Thermal kinetics explained by a first-order model, show an apparent activation energy of 112.3 kJ·mol^{-1}, which is lower compared to other ionic liquids.

1. Introduction

Bio-based and biodegradable polymers represent a promising future for the plastic industry under the current Safe-and-Sustainable by-design of products (E. Commission, 2019; United Nations (UN), 2022; S.-G. European Commission, 2018; C. of the E. U. European Parliament, 2019; European Bioplastics, 2023). In this regard, biopolymers involve a lower environmental impact in contrast to petroleum-based polymers (Pellis et al., 2021), Cosate de Andrade et al. (2016). Though this class accounts for ~1.5 % of the global annual plastic production (Plastics Europe, 2022), its production capacity is estimated to increase from 2.23 MT in 2022 to 6.29 MT in 2027 involving a 5-year period predicted growth rate of more than 180 % (European Bioplastics, 2022). The challenges in this field are focused on the material's performance, long-term stability, and sustainable management of wastes (RameshKumar et al., 2020; J.D. Badia et al., 2017).

Among biopolymers, polylactide (PLA) is a thermoplastic polyester which stands out as a future alternative to traditional plastics such as poly(ethylene terephthalate) (PET) or poly(styrene) (PS), due to its competitive mechanical properties and transformation capabilities (Pang et al., 2010; Moliner et al., 2017). Moreover, its performance can be tailored according to the service and post-service needs through its combination with additives, and fillers or by blending it with other polymers (Wolf et al., 2023; Gil-Castell et al., 2022; J.D. Badia et al., 2017; Gil-Castell et al., 2014; J.D. Badia et al., 2017; Moliner et al., 2018; Gil-Castell et al., 2016; Sepúlveda et al., 2022.

At the end-of-life stage, PLA can be efficiently decomposed in an industrial composting setting (Gil-Castell et al., 2020; O. Gil-Castell et al., 2018), taking about 30–90 days for full mineralization producing CO_2 and water (Lamberti et al., 2020). This fact fulfils the criteria of the circular economy of plastics following cradle-to-cradle schemes. Even though the inherent biodegradability and carbon reintegration into nature could be an appropriate solution for PLA wastes, it certainly loses value in terms of performance when consumption times are relatively low such as packaging or disposable household (J.D. Badia et al., 2017). Even more, there would be an extended need for industrial composting facilities capable of coping with the high number of residues that could come from the plastic waste mainstreams. Finally, a remediation step for

* Corresponding author.
E-mail address: jose.badia@uv.es (J.D. Badia).

https://doi.org/10.1016/j.resconrec.2024.107826
Received 17 May 2024; Received in revised form 8 July 2024; Accepted 15 July 2024
Available online 26 July 2024

soil would be necessary due to acidification during biodegradation Brizga et al. (2020). Consequently, different valorization routes should be used to recover the intrinsic value of the polymers before discarding them towards biological routes, in search of to waste-to-gate schemes.

Literature shows research on mechanical (J.D. Badia et al., 2012; Badia et al., 2011; O. Gil-Castell et al., 2018; Badia et al., 2019; J.D. Badia et al., 2012; J.D. Badia et al., 2012; Badia et al., 2014; Pascual--Jose et al., 2021; Paiva et al., 2024; Pérez-Fonseca et al., 2023), and chemical recycling through pyrolytic (Moliner et al., 2018; J.D. Badia et al., 2012) and solvolytic routes (Solis and Silveira, 2020; McKeown and Jones, 2020; Aryan et al., 2021; Piemonte et al., 2013; Siddiqui et al., 2020; Cristina et al., 2018; Gironi et al., 2016; V. Piemonte and Gironi, 2013) for PLA. Generally, mechanical recycling is applied to reuse PLA in downgraded applications, even though up to two cycles of shredding/injection-extrusion have been demonstrated as feasible (Gil-Castell et al., 2022; Badia and Ribes-Greus, 2016), and upgrading opportunities have been described (Badia and Ribes-Greus, 2016). The combination of recycled and virgin PLA has also shown appropriate performance (O. Gil-Castell et al., 2018). However, since food-contact packaging is a relevant application for PLA, this route is not very exploited, due to likely cross-contamination and the presence of non-intentionally added substances (NIAs) from the consumption-discarding-sorting-reprocessing pathway (Zimmermann et al., 2019; Horodytska et al., 2020). In contrast, chemical recycling permits obtaining the initial building blocks as monomers, oligomers or monomer-related substances, through the depolymerization of the polymer chains by using specific solvents capable of cleaving the functional groups of the backbones, such as the ester group in PLA (McKeown and Jones, 2020; Piemonte et al., 2013; Majgaonkar et al., 2021; Tsuneizumi et al., 2010; S. Zhang et al., 2023). Interestingly, combined (de-re)polymerization strategies are also proposed (Yang et al., 2022).

Chemical recycling of polyesters has been the focus of numerous research in recent years, intending to turn waste into high-value-added chemicals (M. Li and Zhang, 2024; M. Li and Zhang, 2024; S. Zhang et al., 2023; S. Zhang et al., 2023). In particular, for PLA, solvolytic routes have been reported through hydrolysis and alcoholysis, providing lactic acid or methyl/ethyl lactate, respectively (McKeown and Jones, 2020). The solvolysis of PLA usually requires high temperatures and/or strong acid/basic conditions (Elsawy et al., 2017), which makes necessary the use of catalysts for allowing milder conditions, such as alkali halide salts (Liu et al., 2015), metals (Petrus et al., 2016), or ionic liquids (IL) (Song et al., 2013; Song et al., 2019; Liu et al., 2017; Chaudhary and Srivastava, 2023). Commonly used ILs are aprotic ionic liquids (APILs), which stand as liquid salts at ambient temperature, in which their components are tied by ionic forces (Koutsoukos et al., 2022; Ghandi, 2014). They can be obtained by the combination of cations of the family of imidazoliums, pyridiniums, alkylammoniums, phosphoniums or pyrrolidiniums, together with anions such as fluorophosphates, sulfonates, nitrates, acetates or halides (Ye et al., 2013). APILs possess lower vapour pressures than those of volatile organic compounds (VOC) at standard conditions, low toxicity, and suitable biodegradability (Oliveira et al., 2016; Reid et al., 2018). During the chemical recycling of polyesters, the hydrogen of the cationic species of the IL reacts with the carbonyl oxygen C = O of the ester group forming a hydrogen bond and increasing the electric density of the carbon, which is attacked by the oxygen atom of the solvent, e.g., water or alcohol, and subsequently breaks the macromolecule into its main constituents (Zhang et al., 2011). Table 1 gathers previous studies on the chemical recycling of PLA through hydrolysis catalyzed by aprotic ionic liquids, considering operating aspects such as temperature (T), polymer-to-solvent ratio (P/S), polymer-to-ionic liquid ratio (P/IL) and time of operation (t), together with the obtained conversion rate (X_{PLA}).

Alternatively, protic ionic liquids (PILs) have received great interest as metal-free ionic liquid catalysts, given their cost-effectiveness, easy synthesis, and no formation of by-products (Greaves and Drummond, 2008). The protic ionic liquid 2-hydroxyethyl ammonium acetate (2-HEAA) stands out among PILs, with its extensively studied properties (Hosseini et al., 2019; Ghahramani et al., 2020), of relevant interest when applied to different chemistry-related strategies (Kang et al., 2016; Sobhani and Honarmand, 2013; Chavan et al., 2009; Ahfad-Hosseini et al., 2017; Choi and Kwon, 2011; Yuan et al., 2007; Kurnia et al., 2009; Rocha et al., 2017). Notably, the exploration of 2-HEAA as a catalytic agent for the chemical recycling of plastics remains an area yet to be investigated.

Considering the few valorization studies on the chemical recycling of PLA based on the hydrolysis process in combination with ionic liquids, this work aimed to perform the hydrolytic chemical recycling of PLA catalyzed by 2-hydroxyethyl ammonium acetate (2-HEAA) to recover the generated lactic acid into calcium lactate ($Ca(LA)_2$). The particular focus of this study is the maximization of the conversion degree employing a statistical design of experiments, the understanding of the mechanisms of depolymerization induced by 2-HEAA and the determination of the thermal kinetics that govern the solvolytic reaction.

2. Materials and methods

2.1. Materials and reagents

Polylactide (PLA) Ingeo 2003D from Natureworks was used. 2-hydroxyethyl ammonium acetate (2-HEAA) was prepared by a combination of acetic acid (>99.0 %) and ethanolamine (>99.50 %), both provided by Sigma-Aldrich, as described elsewhere (Hosseini et al., 2019; Ghahramani et al., 2020). Calcium carbonate ($CaCO_3$, 99 % analysis grade) was purchased from ThermoFischer Scientific. HPLC-grade water from VWR was used as the hydrolysis medium.

2.2. Hydrolytic chemical recycling of PLA

For the hydrolytic chemical recycling of PLA, 1 g of polymer flakes was put into 40 mL glass vials with threaded plugs, and subjected to the reaction media, composed of H_2O and 2-HEAA. The vials were treated onto an Onilab MS7-H550-Pro magnetic hot plate. Hydrolysis took place at constant temperatures ranging between 120 and 140 °C, under magnetic stirring at 850 rpm, at different times up to 3 h. The unreacted PLA was then removed at ambient temperature by vacuum filtration. Then, the filters were washed with deionized water and dried at 40 °C until constant mass was achieved. The lactic acid (LA) present in the hydrolysis product was converted into calcium lactate ($Ca(LA)_2$) by reaction with calcium carbonate. PLA conversion (X_{PLA}) was calculated

Table 1
Previous studies on the chemical recycling of PLA through hydrolysis catalyzed by aprotic ionic liquids.

Ref.	PLA	Cationic species	Anionic species	T (°C)	P/S (g:g)	P/IL	t (h)	X_{PLA} (%)
(X. Song et al., 2014)	Shenzhen ESUN Industrial Co., Ltd.	[HSO_3-pmim]	[HSO_4]	130	2:3	1:0.5 (g:g)	2	85.21
		[Bmim]	[Cl]				2	9.56
		[Bmim]	[OAc]				2	93.93
		[Bmim]	[OAc]				2	90.86
		[Emim]	[NTf_2]				2	7.36
(Jiang et al., 2015)	PLLAr	[Bmim]	[Cl-$SnCl_2$]	200	0.37:1	1:10^{-3} (mol:mol)	2	57–59

according to Eq. (1), while hydrolysis product yield (R_{LA}) was calculated by Eq. (2),

$$X_{PLA}(\%) = \left(\frac{m_{0\ PLA} - m_{f\ PLA}}{m_{0\ PLA}}\right) \times 100 \quad (1)$$

$$R_{LA}(\%) = \left(\frac{\frac{m_{Ca(LA)_2}}{Mw_{Ca(LA)_2}} \cdot 2}{\frac{m_{converted\ PLA}}{Mw_{LA}}}\right) \times 100 \quad (2)$$

where $m_{0\ PLA}$, $m_{f\ PLA}$ are the initial and final masses of PLA (g), respectively; $m_{Ca(LA)}$ is the final mass of the calcium lactate (g); $Mw_{Ca(LA)2}$ is the molar mass of calcium lactate (218.22 g·mol^{-1}); and Mw_{LA} is the molar mass of the lactic acid (90.08 g·mol^{-1}).

The maximization of the PLA conversion (X_{PLA}) was carried out with a comprehensive statistical strategy (Mukerjee and Wu, 2006), considering the selected parameters: (*i*) temperature (T) {120, 130 and 140 °C}, chosen between the cold crystallization temperature and the melting temperature of PLA (Hakkarainen and Finne-Wistrand, 2011); (*ii*) plastic-to-solvent mass ratio (P/S) {1:6, 1:8 and 1:10, PLA:H_2O, g:g}; and (*iii*) plastic-to-ionic liquid mass ratio (P/IL) {1:0.5, 1:1.5 and 1:2.5, PLA:2-HEAA, g:g}, following a statistical full 2^3 factorial Design of Experiments (DoE), described in the **Table S1** of the Supplementary Material. The DoE approached the behavior of the system by the polynomial expression shown in Eq. (3), where β_0 is the offset parameter, β_i are linear effects, β_{ij} are interaction effects, β_{ii} are the quadratic effects and X_i, X_{ij}, X_{ii} ($i = 1,2,3, j = 1,2,3, i \neq j$) are the factors {($X_i$: T, P/S, P/IL); ($X_{ij}$: T·P/S, T·P/IL, P/S·P/IL); (X_{ii}: T·T, P/S·PS, P/IL·P/IL)} of the analysis.

$$X_{PLA}\ (\%) = \beta_0 + \sum \beta_i \cdot X_i + \sum \beta_{ij} \cdot X_{ij} + \sum \beta_{ii} \cdot X_{ii} \quad (3)$$

The approximated molar ratios of the 2-HEAA to PLA were 0.3, 0.9 and 1.5 for mass proportions (g:g; IL:PLA) of 0.5:1, 1.5:1 and 2.5:1, respectively.

2.3. Thermal kinetics of the hydrolysis reaction

The energy requirements of the hydrolysis reaction of PLA were evaluated according to the results of the maximization section. The P/S ratio was set at 1:6 and the P/IL at 1:2.5. The temperature ranged between 120 and 140 °C by 5 °C steps. Reaction times were set at 30, 60, 90, 120, 150, and 180 min. A first-order model, as shown in Eq. (4), was considered for the modelling of the conversion of PLA (X_{PLA}), being k (min^{-1}) the rate constant of the reaction.

$$\ln \frac{1}{1 - X_{PLA}} = k \cdot t \quad (4)$$

The apparent activation energy (E_a) was obtained from the evolution of the reaction constant with temperature, according to the linearized Arrhenius model shown in Eq. (5),

$$\ln k = \ln A - \frac{E_a}{R \cdot T} \quad (5)$$

where A is the pre-exponential factor, R is the ideal gas constant (8.31 J·K^{-1}·mol^{-1}) and T is the temperature (K).

2.4. Analytical techniques

Nuclear Magnetic Resonance (NMR) ^{1}H spectra were acquired in $CDCl_3$ solution at 300.13 MHz on a Bruker 300 Avance III HD using a 5 mm BBF probe head equipped with Z gradients. The samples were measured at 25 °C. High-Resolution Mass Spectrometry (HRMS) was performed on a Sciex, TRIPLETOFT5600.

Attenuated total reflection (ATR) Fourier transform infrared (FTIR) spectra were recorded by an FTIR-ATR Agilent Cary 630 spectrometer. Measurements were conducted from 4000 – 650 cm^{-1} at room temperature. 64 co-added spectra were recorded for each specimen at a resolution of 4 cm^{-1} with a spacing of 1 cm^{-1}. Spectra were normalized to the 1454 cm^{-1} peak before any data processing, which is usually used as an internal standard (J.D. Badia et al., 2012), and it is useful to correct possible variations arising from defects in surface quality or sample positioning.

Thermogravimetric analyses (TGA) were conducted in a Perkin Elmer TGA 7. Approximately 10 mg of specimens were placed in 70 μL alumina pans and analyzed under an inert atmosphere of Ar with a flow rate of 50 mL·min^{-1}, from 30 – 800 °C, at a heating rate of 10 °C·min^{-1}. The samples were characterized with the aid of the software TRIOS, at least in triplicates, and the averages were taken as representative values.

Differential scanning calorimetry (DSC) analyses were carried out using a TA Instruments DSQ Q20. Approximately 5 mg of specimens were placed in 40 μL aluminium pans, which were sealed and pierced on top. A heating/cooling/heating program with a 10 °C·min^{-1} rate was applied in the temperature range between 30 °C and 200 °C under an inert atmosphere of N_2 with a gas flow of 50 mL·min^{-1}. The samples were characterized with the aid of the software TRIOS, at least in triplicates, and the averages were taken as representative values.

Data treatment and graphing have been carried out with OriginPro 2023 V10.0.0.154. Statistical analyses were carried out with the aid of Minitab 19.1.

3. Results and discussion

The hydrolytic conversion of PLA into LA, subsequently transformed into $Ca(LA)_2$ driven by 2-HEAA as catalytic co-solvent was approached from different perspectives, to test its validity to adhere to the foreseen performance criteria under a waste-to-gate circular model. An initial deep investigation into the mechanism of PLA into LA driven by 2-HEAA was performed. Subsequently, the relative effects of each experimental factor of the reaction triplet, i.e. {T, P/S, P/IL} governing the hydrolytic reaction were tested. Consequently, a maximization procedure was carried out to set up the most appropriate values for the reaction triplet to promote the conversion of PLA. Finally, the thermal kinetics were tested to benchmark the energy requirements of the reaction with current state-of-the-art using other catalysts.

3.1. Mechanistic route for the chemical recycling of PLA into $Ca(LA)_2$

The mechanistic route for evaluating the chemical recycling of PLA was conducted from multiple and complementary perspectives. The characterization of the hydrolysis product was conducted through spectroscopic and thermal analysis strategies that allowed the identification of the obtained compound after PLA hydrolysis and subsequent precipitation.

Fig. 1**a** shows the ^{1}H NMR spectra of solubilized PLA sample (top) and precipitated $Ca(LA)_2$ (bottom). As it can be observed, PLA proton atom signals are straightforwardly detected, i.e., a quadruplet around 5.2 ppm and a doublet near 1.6 ppm, which have a 1/3 integration ratio. Lactate presents a similar doublet (CH_3) and quadruplet (CH) pair, at 1.50 and 4.38 ppm, respectively. The significant difference in the CH between PLA and $Ca(LA)_2$ is explained by the presence of an OH group instead of an ester. The $Ca(LA)_2$ sample was obtained by precipitation with calcium carbonate as a metal source. As can be seen, traces of PLA are present in this spectrum. It is worth mentioning that 2-HEAA could be recovered after the reaction showing no trace of PLA or LA (Cui et al., 2016).

Fig. 1**b** represents the FTIR spectra of the residue obtained from the first cycle, which shows all the characteristic peaks of $Ca(LA)_2$. The broad band at high wavenumber, with a peak around 3210 cm^{-1} is due to the hydroxyl stretching vibration. Moreover, the peaks at 2990 and 2940 cm^{-1} can be correlated to the symmetric and asymmetric vibration of CH_3. The intense absorption band occurring at approximately 1570 cm^{-1}

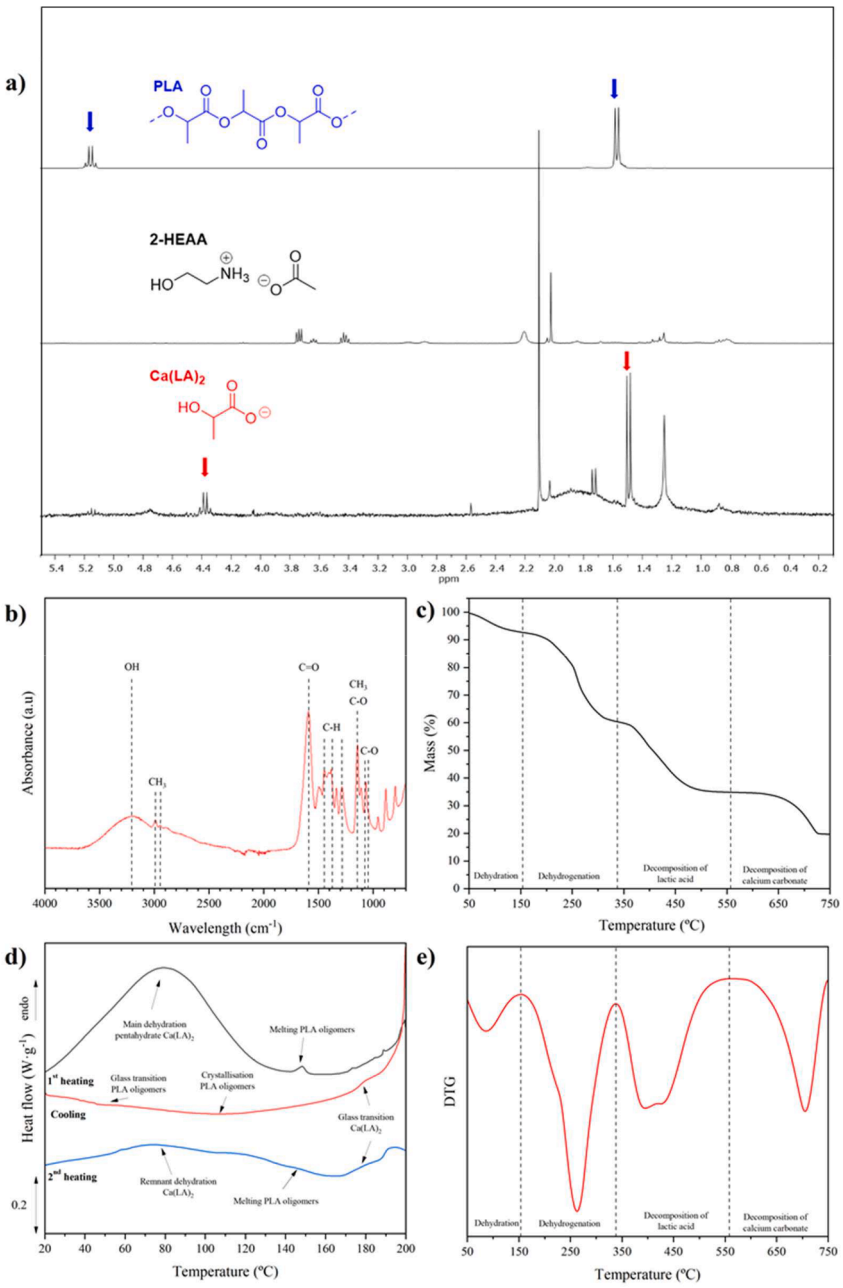

Fig. 1. (a) ^{1}H NMR spectra of PLA (top), recovered 2-HEAA (middle), and $Ca(LA)_2$ (bottom); **(b)** FTIR spectra of $Ca(LA)_2$; **(c)** Differential scanning calorimetry thermograms for the first heating, cooling and second heating of $Ca(LA)_2$; **(d)** Thermogravimetric thermogram of $Ca(LA)_2$; and **(e)** Derivative thermogravimetric thermogram of $Ca(LA)_2$.

represents a C = O stretching vibration. The peaks in the range between 1430 cm^{-1} and 1360 cm^{-1} indicate C–H both symmetric and asymmetric bending phenomena, while the band located at 1390 cm^{-1} is ascribed to hydroxyl bending motions. At 1270 cm^{-1}, the C—H bending vibration could be identified. The significant peak found at 1120 cm^{-1} is the result of the sum of the rocking absorption of methyl groups and the stretching vibration of the C–O bond in the alcohol. Additionally, bands at 1090 and 1047 cm^{-1} are also characteristic of the C–O in the alcohol. All these bands correlate well with those reported in the literature for lactates (Hosseini et al., 2019; Ghahramani et al., 2020; Kang et al., 2016) and allow identification of the composition of the obtained compound as $Ca(LA)_2$.

The obtained product was further characterized, according to its thermal performance. Thermogravimetric analysis was thus conducted, which obtained thermogram and first derivative curve (DTG) are shown in Fig. 1**d** and 1**e**. The thermogravimetric trace revealed four main subsequent mass-loss steps as a function of temperature, typical for $Ca(LA)_2$ (Kiran-Yildirim et al., 2018). First, one-step dehydration was identified from the onset of the analysis up until 150 °C, involving a mass-loss percentage of 7.56 % which corresponds to 4.95 equivalents of water. The remaining 0.05 equivalents of water may have been released preceding data recording below 50 °C. This process was visible in the DTG curve with a peak temperature of ~85 °C, where the dehydration rate was maximum. The observed dehydration performance is coherent with the previous reports for the pentahydrate form of $Ca(LA)_2$ (Sakata et al., 2005; De Maere D'aertrycke et al., 2020; Polat, 2022). Afterwards, the decomposition of anhydrate $Ca(LA)_2$ began, with a process comprising a mass loss percentage of ~32 % from 160 to 335 °C, and a maximum decomposition rate at ~263 °C. This process was ascribed to the elimination of ethyl 2-hydroxypropanoate (Seesanong et al., 2022).

The following step above 340 °C and up to 550 °C involved a ~25 % mass-loss, where lactic acid was completely decomposed, leaving as a result calcium carbonate. Above 630 °C, the calcination of calcium carbonate produced calcium oxide and carbon dioxide (Li et al., 2017), with a mass loss percentage of ~15 % and a maximum decomposition rate at ~715 °C. Therefore, at the end of the thermogravimetric assay, a solid residue representing a mass percentage of 20 % was assumed to be mainly calcium oxide, which is a thermally stable substance with a reported melting point of 2572 °C (Yang et al., 2022).

The thermal properties were complementarily assessed through differential scanning calorimetry, which sequentially obtained first heating, cooling and second heating scans are shown in Fig. 1**c**. During the first heating, a wide endothermal transition occurring from 20 – 150 °C was identified, with a peak at ~80 °C and an estimated heat of reaction of ~135 $J{\cdot}g^{-1}$. In line with previous findings and other studies in the literature (De Maere D'aertrycke et al., 2020), it is due to the main dehydration stage of the pentahydrate form of $Ca(LA)_2$. At higher temperatures, a minor endothermal transition was observed, with a peak at ~148 °C. Given the absence of mass loss events at this temperature in the thermogravimetric trace, and its correlation in the low range of the melting of polylactide (150–160 °C, (Sin et al., 2013)), the presence of a small fraction of remnant hydrolyzed crystallized PLA oligomers can be assumed. Further temperature increase suggested the beginning of the thermal decomposition process of $Ca(LA)_2$ above ~170 °C. During cooling, the glass transition of anhydrate $Ca(LA)_2$ was identified in the vicinities of ~178 °C, in agreement with the literature (De Maere D'aertrycke et al., 2020). Concerning PLA oligomers, a wide endothermal crystallization event with a peak at ~110 °C together with the glass transition in the range between 35 and 45 °C could be intuited. Further heating showed a thermogram with multiple small shoulders, that could be correlated to the thermal events found during previous heating and cooling segments. First, the evaporation of remnant water molecules in a partially hydrated $Ca(LA)_2$ was detected. The use of a heating rate of 10 $°C{\cdot}min^{-1}$ during the first heating may have not allowed for complete water volatilization, which was then released during the second heating. The shoulder at ~150 °C was due to the melting of PLA oligomers and finally, the glass transition of $Ca(LA)_2$ was corroborated at ~176 °C.

Altogether, the obtained compound was identified as the pentahydrate form of $Ca(LA)_2$, whose production mechanistic route can be appreciated in Fig. 2. The polymer degradation starts with a simple carbonyl protonation. 2-HEAA acts as a Brønsted acid and activates the ester systems being able to react with nucleophiles. The amino ethanol attacks the activated carbonyl through an addition/elimination mechanism. This process results in an amide that is transformed into acid in the presence of water and afterwards participates in further chain cleavages. In HRMS a compound could identified (as a trace) as the amide derived from LA and amino ethanol. This mechanism is also in agreement with the action of 2-HEAA as a homogeneous catalytic co-solvent of other widely used polyester such as poly(ethylene terephthalate) (PET) (Badia et al., 2024).

3.2. *Individual and combined influence of factors on chemical recycling of PLA*

The direct and combined impact of each factor (T, P/S and P/IL) on the hydrolytic conversion of PLA were estimated following a full 2^3 factorial statistical DoE. At stage 1, individual (T, P/S, P/IL), interaction (T·P/IL, T·P/S, P/IL·P/S) and quadratic (T·T, P/S·P/S, P/IL·P/IL) coefficients were initially tested. **Table S2** in the Supplementary Material summarizes the different stages of analysis of this section and will be used as a recall along the discussion. The significance of each coefficient in the equations was determined by the Fischer-Snedecor *F*-test and *p-value*. A term was considered statistically significant when its corresponding *p-value* was lower than 0.05 at a 95 % confidence level. At stage 1, the significance of quadratic coefficients was not statistically relevant and was therefore removed from the model. This means that no curved surface was expected to offer a maximum at the experimental conditions of the experiment. At stage 2, individual and interaction factors were considered. The Pareto chart, with the indication of the Fischer-Snedecor *F-value* and significance *p-value* obtained from the analysis of variance, is shown in Fig. 3**a**. The plot shows that the larger the *F-value*, the higher the effect of the factor on the response. It was found that individual effects (T, P/S, P/IL – $F = 337.08$) were ~100 times more relevant than the interaction effects (T·P/S, T·P/IL, P/S·P/IL – $F = 3.65$). The boundary value of significance for the standardized effect (2.03), as obtained per Student's t-distribution, indicated the significance of factors. The most relevant factors were the temperature (T) and the plastic-to-ionic liquid ratio (P/IL), followed by the interaction of T·P/IL and the plastic-to-solvent P/S ratio, in similar terms. The interactions T·P/S and P/IL·P/S were not considered statistically relevant, due to *p-value* < 0.05.

In order to give a closer look at the impact of each parameter on the conversion, the Main Effects Plot (MEP) for the individual parameters T,

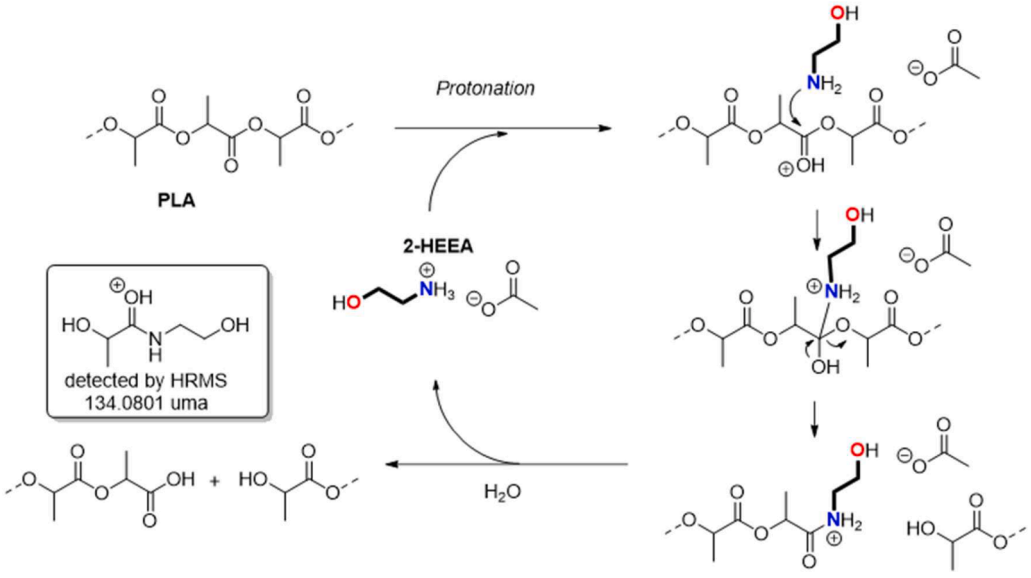

Fig. 2. Predicted reaction mechanism of the hydrolysis of PLA using 2-HEAA as a catalytic co-solvent.

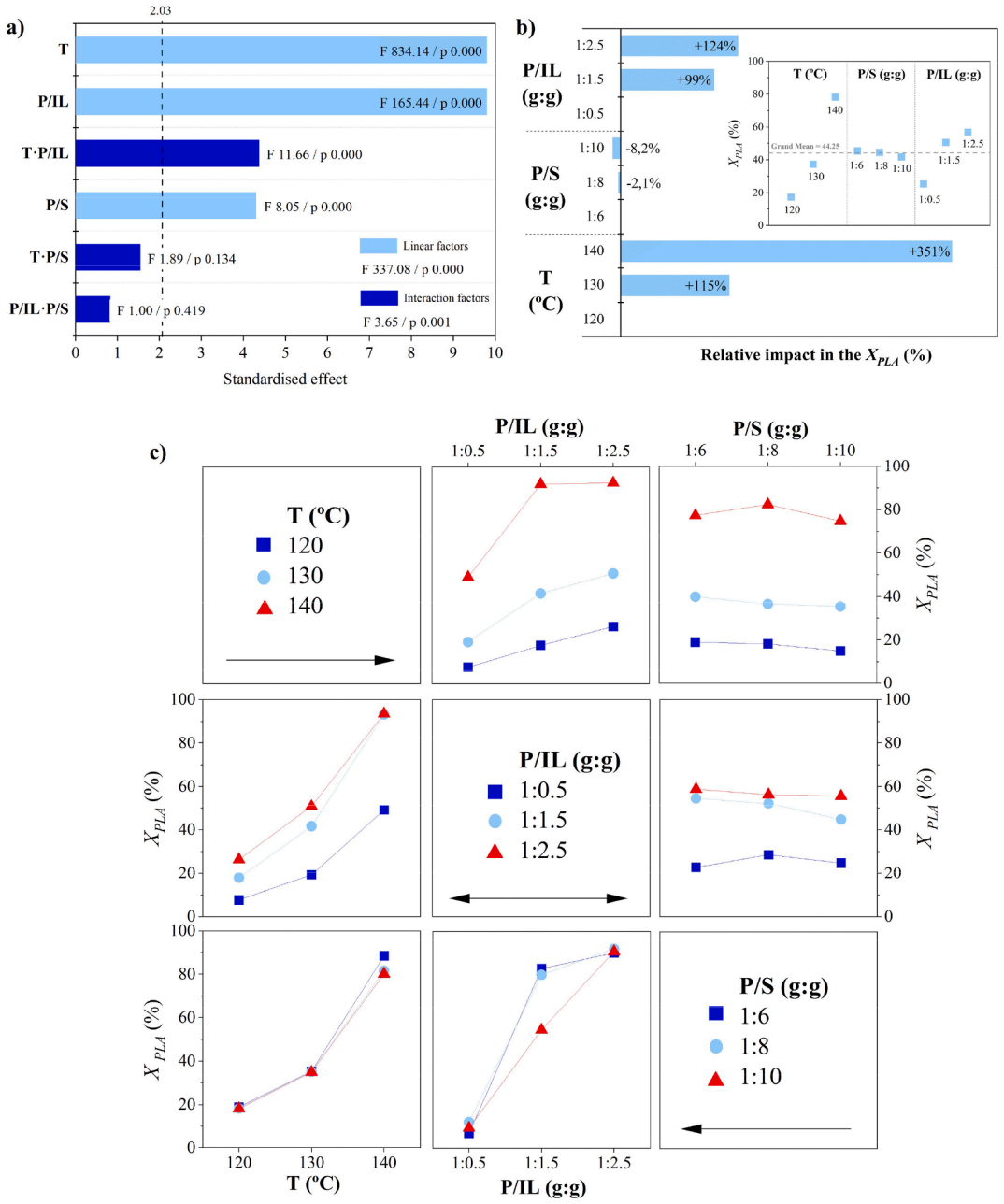

Fig. 3. **(a)** Pareto plot of the standardized effects of the proposed regression model for the hydrolysis reaction of PLA aided by 2-HEAA. *F* stands for the Fischer-Snedecor *F-value* and *p* stands for the *p-value* of statistical significance of analysis of variance. Significance level = 2.03; **(b)** Relative impact of each experimental factor in the conversion of PLA (X_{PLA}). Inset: Main Effects Plot (MEF) of the influence of temperature (T), polymer-to-solvent ratio (P/S) and polymer-to-ionic liquid ratio (P/IL), as obtained from the full 2^3 factorial design of experiments; and **(c)** Interaction Effects Plot (IEF) of the influence of temperature (T), polymer-to-solvent ratio (P/S) and polymer-to-ionic liquid ratio (P/IL) on the conversion of PLA (X_{PLA}), as obtained from the full 2^3 factorial design of experiments. The axes, scales and labels are shared in the horizontal and vertical directions.

P/S and P/IL, is shown in the inset of Fig. 3**b**. Each point of the MEP shows the average of the experiments performed at a single condition. For instance, the results at 130 °C are the average of all experiments performed at 130 °C for all P/S and P/IL combinations. The horizontal line around ~46 % shows the grand mean, which is the average conversion from all performed experiments. This centred value is helpful to evaluate the relative influence of each factor over a wide range of experimental conditions. Fig. 3**b** shows the relative impact of each factor, taking as a baseline the lower levels of each one.

In addition, the Interaction Effects Plot (IEF) for the interaction parameters T·P/S, P/S·P/IL and T·P/IL is shown in Fig. 3**c**, to help visualize both the statistical significance of these parameters and their impact on the response. Several observations can be drawn from the study of both MEF and IEF plots, as follows:

(i) Concerning temperature (T), the higher it was, the higher the conversion was obtained, being that of 140 °C the one offering larger averaged conversions. A relative 115 % increase in conversion was obtained when moving from 120 °C to 130 °C, whereas a subsequent 10 °C increase provided up to a 351 % increase. It is relevant to mention that higher temperatures are experimentally restricted, to avoid partial fusion of PLA, which may start at temperatures around 150 °C (J.D. Badia et al., 2012). This value is relatively lower than others reported, between 180

°C and 220 °C for catalysts based on metal salts, alkalis, or some APILs, which may imply energy savings for a scaled-up technology (McKeown and Jones, 2020; Payne and Jones, 2021). Only in the case of [Bmim][OAc] APIL, a slightly lower temperature is reported (130 °C) but using a higher P/S ratio and achieving a lower conversion (McKeown and Jones, 2020; X. Song et al., 2014).

(ii) Regarding the P/S factor (PLA:H_2O ratio), it acted in an inversely proportional manner on the conversion. This effect agrees with other studies in which the amount of solvent is not necessary to be very high in relation to the amount of plastic. For instance, the increase of P/S proportion using the APIL [Bmim][OAc] as catalyst from 2:1 – 6:1 increases the conversion a 10 %, but the increase of P/S relation from 6:1 – 8:1 entails a rise of 1 % of conversion of PLA (McKeown and Jones, 2020). In any case, the P/S was not as intense in terms of influence on the conversion, in contrast to T and P/IL. From the point of view of a further scale-up, positive aspects such as solvent savings and reduced volume reactors can be pursued.

(iii) The P/IL factor (PLA:2-HEAA ratio) showed a direct proportionality for the PLA conversion, which indicates that the presence of the 2-HEAA was relevant. Indeed, conversions without 2-HEAA ranged around 5–20 %. It is important to remark on the reduction of slope from the segments connecting the averages at experiments from P/IL 1:0.5–1:1.5 (+99 % increase) to 1:1.5–1:2.5 (+124 % increase).

(iv) As for the combined effect of factors shown in Fig. 3**c**, the interaction of T and P/S, and the interactions of P/S and P/IL were not relevant. When it comes to the interaction between T and P/IL, the slope of the variation of means was higher with every increase of T at a fixed P/IL or P/IL at a fixed T. Concerning T, it is necessary to heat up to 140 °C to get high conversions. Regarding P/IL, with a focus on further scale-up, a P/IL ratio of 1:1.5 would be a reasonable option for 2-HEAA savings, with similar results as those shown by the experiments at a P/IL ratio of 1:2.5.

3.3. Maximization of chemical recycling

After considering all the observations, a regression model was proposed bearing in mind only the statistically relevant coefficients, i.e., T, P/S, P/IL and T·P/IL, in order to simplify the final equation for better operativity. The model is shown in Eq. (6), with a regression coefficient of 94.16 %, being valid in the experimental windows comprised within T ∈ [120,140] (°C), P/S ∈ [1:6, 1:8] (g of P/S), and P/IL ∈ [1:0.5, 1:2.5] (g of P/IL), at a 95 % level of confidence. Fig. 4**a** shows the 3D plot of the proposed regression model.

$$X_{PLA}(\%) = 0.3684 \cdot T - 186.9 \cdot \frac{P}{IL} - 2.77 \cdot \frac{P}{S} + 1.541 \cdot \left(T \cdot \frac{P}{IL}\right) - 7 \qquad (6)$$

Maximization results in this section involved the suggestion of three options with the highest conversions of PLA, all of them at 140 °C with different proportions of P/IL (1:2.5 and 1:1.5) and P/S (1:6 and 1:8), with conversions gathered in **Table S3** of the Supplementary Material. First, from an environmental perspective, it is relevant to remark that the fewer reagents are used the lower the environmental impact the process will have, especially those that are consumed during the hydrolytic valorization of PLA. In this regard, a higher solvent proportion results in a lower conversion of PLA with the subsequent increase of the process costs due to higher solvent consumption. Consequently, a condition with a P/S of 1:8 can be rejected as the optimal condition, as it considers a higher solvent percentage with the lowest conversion of PLA (94.0 %). Next, considering that the 2-HEAA could be recovered after the hydrolytic reaction showing no trace of PLA or LA, the P/IL proportion with the highest conversion of PLA should be selected. Altogether, the most promising choice was found with a reaction triplet

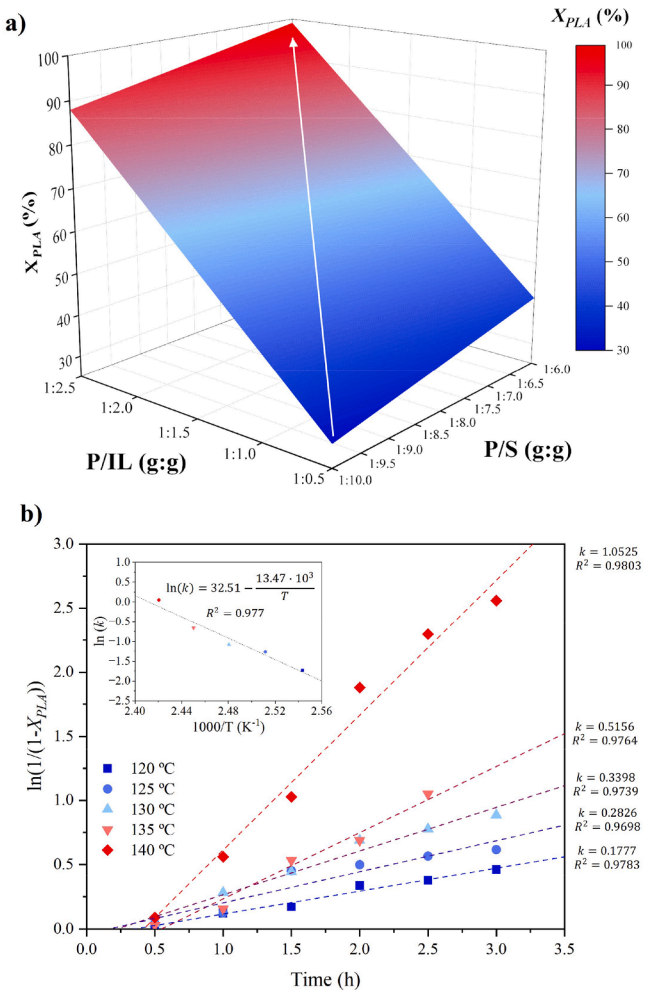

Fig. 4. (a) 3D plot of the regression model for the maximization of conversion of PLA. Experimental conditions were set at T = 140 °C; and **(b)** depolymerization rate of the hydrolysis process following the first-order reaction. Inset: First-order Arrhenius plot of the hydrolysis process. Note that error bars are not included for the sake of clarity, the standard deviation for the results is approximately 1 unit, and the units of k are s^{-1}.

involving a T of 140 °C, a P/S ratio of 1:6, and a P/IL proportion of 1:2.5. Considering that other studies in the literature reported hydrolytic conversions of PLA above 90 % with other catalysts (O. Gil-Castell et al., 2018; Piemonte et al., 2013; Siddiqui et al., 2020; Cristina et al., 2018; Gironi et al., 2016), comparable hydrolytic performance using 2-HEAA as the catalytic co-solvent can be achieved. For the selected optimal system, the recovery yield relative to the initial PLA was 72 %. Considering that the $Ca(LA)_2$ recovery sequence involves a reaction step with calcium carbonate, cooling, precipitation and two-step filtration of calcium lactate, a reduction in yield compared to the pure hydrolytic stage may be expected. The optimization of this process may result in higher effective recovery yields.

3.4. Thermal kinetics of PLA conversion

The kinetic study of PLA hydrolysis reaction under the presence of 2-HEAA was performed to approach its energy requirements. For this purpose, five temperatures were selected, ranging from 120 to 140 °C. P/S and P/IL proportions were selected according to maximization conditions of the chemical recycling of PLA found in the previous section, i.e., P/S = 1:6, and P/IL=1:2.5. In line with other authors (X. Song et al., 2014; V. Piemonte and Gironi, 2013; Codari et al., 2012; Speranza et al., 2014; Tsuji et al., 2003; Mohd-Adnan et al., 2008), the

depolymerization kinetics of PLA was considered to be first-order. Hence, a first-order model shown in Eq. (4) was applied, whereas the linearized Arrhenius model, shown in Eq. (5), was applied to obtain the apparent activation energy (E_a) from fitting the evolution of the reaction rate constant with temperature.

The effect of the reaction temperature on the conversion rate of PLA −expressed as $\ln(1/(1-X_{PLA}))$− is shown in Fig. 4**b**, which includes linear fittings to the experimental data with their corresponding fitted reaction rate constant values (k) and correlative coefficients (R^2). As expected, the higher the temperature, the higher the conversion rate, which increased from 0.1777s^{-1} at 120 °C to 1.0525 s^{-1} at 140 °C. All linear fittings revealed high values for the correlative coefficients, above 0.97. Therefore, it can be inferred that the hydrolytic reaction of PLA under the presence of 2-HEAA can be certainly governed by a first-order kinetic model.

The reaction rate constant values (k) yielded by the linear regression analyses were afterwards used to generate the Arrhenius plot of the hydrolysis process based on the first-order kinetic model, shown in the inset of Fig. 4**b**. This Arrhenius plot allowed to calculate the apparent activation energy (E_a) from the slope of the curve's equation, whereas the pre-exponential factor (A) value was directly retrieved from its intercept. The resulting calculated activation energy was 112.3 kJ·mol^{-1} and the A value was $1.4{\cdot}10^{14}$.

For comparison purposes, Table 2 gathers other kinetic analyses reported in the literature for the heterogeneous solvolysis of PLA in the solid state. In terms of hydrolysis, previous works suggest that the activation energy is somewhat higher at 133.9 kJ·mol^{-1} but in this case [Bmim][OAc] was used as a catalyst (X. Song et al., 2014), where the conclusion may be drawn that 2-HEAA is a more effective agent to catalyze the hydrolytic valorization of PLA. Other studies suggested that the activation energy is lower if the process is altered in the way of making the system into a methanolysis process (Badia and Ribes-Greus, 2016; Zimmermann et al., 2019).

4. Conclusions

Solvolytic chemical recycling of PLA was achieved through the hydrolytic conversion into lactic acid and ultimately into calcium lactate under a waste-to-gate circular model, with a special focus on determining the potential of 2-hydroxyethyl ammonium acetate (2-HEAA) as a homogeneous catalytic co-solvent.

This reaction was proven to be mechanistically induced by the attack of the amino ethanol group of 2-HEAA to the carbonyl group of PLA, through an addition/elimination process. Interestingly, the 2-HEAA could be recovered after the reaction showing no trace of PLA or LA, which permits its reutilization in further recycling steps.

The hydrolysis was performed at temperature (T) ϵ {120, 130, 140 °C}, plastic-to-solvent mass ratio (P/S) ϵ {1:6, 1:8, 1:10 g:g} and plastic-to-ionic liquid mass ratio (P/IL) ϵ {1:0.5, 1:1.5, 1:2.5 g:g}. A full 2^3 factorial DoE demonstrated that quadratic T^2, P/S^2, PIL^2 factors and interaction T·P/S and P/S·P/IL factors were not statistically significant. An equation based on individual T, P/S and P/IL factors, together with the interaction T·P/IL factor explained the experimental results with a high regression coefficient. T was the most relevant factor, and it can be used at values between 120 and 140 °C, which are milder temperatures than those used with other metal-based or alkali-based catalysts, which positively encompasses energy savings. The amount of P/S was statistically relevant but, in terms of cost-efficiency, it is not necessary to use a high solvent proportion, which reduces the consumption of reagents. Finally, the P/IL proportion was also relevant, achieving better conversions with a higher amount of ionic liquid. However, the aforementioned capability of recovery without traces and reuse for other recycling steps, makes it beneficial. In general, the best reaction triplet was formed by a temperature of 140 °C, a mass ratio between PLA and water P/S of 1:6, and a mass ratio between PLA and 2-HEAA P/IL of 1:2.5.

Also, thermal kinetics were approached, and a first-order model, with an apparent activation energy of 112.3 kJ·mol^{-1}, pointed out mild energy requirements, in contrast to other metal-based and imidazole-based ionic liquids.

As a general conclusion, the results show the potential of 2-HEAA as a catalytic co-solvent for the solvolytic recycling of PLA via hydrolysis, due to aspects such as the use of moderately low conversion temperatures, minimum plastic-to-solvent ratios and reasonable plastic-to-ionic liquid ratios, which can represent a window of opportunity for waste-to-gate circular pathways of future polylactide wastes. More practical research, conducted in settings closer to industrial-scale processes, is necessary to ensure accuracy and applicability in a real-world scenario.

CRediT authorship contribution statement

A. Cháfer: Writing – review & editing, Visualization, Validation, Supervision, Software, Resources, Methodology, Investigation, Formal analysis, Data curation, Conceptualization. **O. Gil-Castell:** Writing – review & editing, Writing – original draft, Visualization, Validation, Software, Formal analysis, Data curation. **A. Björling:** Writing – original draft, Investigation, Formal analysis, Data curation. **R. Ballesteros-Garrido:** Writing – review & editing, Writing – original draft, Validation, Methodology, Investigation, Data curation. **J.P. Cerisuelo-Ferriols:** Writing – original draft, Visualization, Validation, Investigation, Formal analysis. **J.D. Badia:** Writing – review & editing, Writing – original draft, Visualization, Validation, Supervision, Software, Resources, Project administration, Methodology, Investigation, Funding acquisition, Formal analysis, Data curation, Conceptualization.

Declaration of competing interest

The authors declare the following financial interests/personal relationships which may be considered as potential competing interests:

J.D. Badia reports financial support was provided by Government of

Table 2
Kinetic analyses of the heterogeneous solvolysis of PLA in the solid state reported in the literature ordered following an increasing E_a sequence. Data from the current study is shown in bold.

Shape	Solvent	Catalyst	T (°C)	E_a (kJ·mol^{-1})	Model assumption	Ref.
Pellet (3.0 × 2.5 mm)	Methanol	[Bmim]$FeCl_4$	100–125	21.28	First order	(Liu et al., 2017)
Pellet (3.0 × 2.5 mm)	Methanol	$FeCl_3$	110–135	32.41	First order	(Liu et al., 2015)
Pellet (3.0 × 2.5 mm)	Methanol	[Bmim][OAc]	90–115	38.29	First order	(Song et al., 2013)
Beads (3–5 mm)	MeOH+THF	Zn(II) complex	40–130	39–65	First order	(Román-Ramírez et al., 2019)
Particles (1–10 mm)	Methanol	Zn(II) complex	70–110	40.80	First order	(Román-Ramírez et al., 2020)
Pellet (3.0 × 2.5 mm)	Methanol	[HSO_3-pmim][HSO_4]	90–115	47.01	First order	(X. Song et al., 2014)
Pellet (3.0 × 2.5 mm)	Steam (saturated)	–	180–250 (molten)	51.40	First order	(Tsuji et al., 2003)
Pellet (3.0 × 2.5 mm)	Water (moisture)	–	180–220 (molten)	60.94	First order	(Speranza et al., 2014)
Pellet (3.92 × 3.48 mm)	Steam (saturated)	–	100–130	87.20	First order	(Mohd-Adnan et al., 2008)
Pellet (1 × 4 mm)	**Water**	**2-HEAA**	**120–140**	**112.30**	**First order**	**Present study**
Pellet (3.0 × 2.5 mm)	Water	[Bmim][OAc]	120–135	133.90	First order	(X. Song et al., 2014)

Valencia. If there are other authors, they declare that they have no known competing financial interests or personal relationships that could have appeared to influence the work reported in this paper.

Data availability

Data will be made available on request.

Acknowledgements

This work was funded by Generalitat Valenciana, Spain, through the projects CRESOL [GV/2021/011] and CIRC4SKILLS [EGJID/2021/237]. The funding source played no role in any aspect related to this research paper. C. Almonacil is thanked for lab assistance. Technical support from Central Services for Experimental Research (SCSIE) and the Institute of Material Science (ICMUV) of the Universitat de València is also recognized.

Supplementary materials

Supplementary material associated with this article can be found, in the online version, at doi:10.1016/j.resconrec.2024.107826.

References

Ahfad-Hosseini, H.R., Bagheri, H., Amidi, S., 2017. Ionic liquid-assisted synthesis of celexocib using tris-(2-hydroxyethyl) ammonium acetate as an efficient and reusable catalyst. Iran. J. Pharm. Res. 16 (1), 158–164 [Online]. Available. http://www.ncbi.nlm.nih.gov/pubmed/28496471.

Aryan, V., Maga, D., Majgaonkar, P., Hanich, R., 2021. Valorisation of polylactic acid (PLA) waste: a comparative life cycle assessment of various solvent-based chemical recycling technologies. Resour. Conserv. Recycl. 172, 105670 https://doi.org/10.1016/J.RESCONREC.2021.105670. Sep.

Badia, J.D., et al., 2014. Dielectric spectroscopy of reprocessed polylactide. Polym. Degrad. Stab. 107, 21–27. https://doi.org/10.1016/j.polymdegradstab.2014.04.023. Sep.

Badia, J.D., et al., 2017a. Effect of sisal and hydrothermal ageing on the dielectric behaviour of polylactide/sisal biocomposites. Compos. Sci. Technol. 149, 1–10.

Badia, J.D., Ballesteros-Garrido, R., Gamir-Cobacho, A., Gil-Castell, O., Cháfer, A., 2024. Chemical recycling of post-consumer poly(ethylene terephthalate) (PET) driven by the protic ionic liquid 2-HEAA: performance, kinetics and mechanism. J. Environ. Chem. Eng. 12 (4), 113134 https://doi.org/10.1016/J.JECE.2024.113134. Aug.

Badia, J.D., Gil-Castell, O., Ribes-Greus, A., 2017b. Long-term properties and end-of-life of polymers from renewable resources. Polym. Degrad. Stab. 137, 35–57. https://doi.org/10.1016/j.polymdegradstab.2017.01.002.

Badia, J.D., Gil-Castell, Ó., Teruel-Juanes, R., Ribes-Greus, A., 2019. Recycling of polylactide. Reference Module in Mater. Sc. Mater. Eng. https://doi.org/10.1016/B978-0-12-803581-8.10569-7. Jan.

Badia, J.D., Ribes-Greus, A., 2016. Mechanical recycling of polylactide, upgrading trends and combination of valorization techniques. Eur. Polym. J. 84, 22–39. https://doi.org/10.1016/j.eurpolymj.2016.09.005.

Badia, J.D., Santonja-Blasco, L., Martínez-Felipe, A., Ribes-Greus, A., 2012a. A methodology to assess the energetic valorization of bio-based polymers from the packaging industry: pyrolysis of reprocessed polylactide. Bioresour. Technol. 111, 468–475. https://doi.org/10.1016/j.biortech.2012.02.013. May.

Badia, J.D., Santonja-Blasco, L., Martínez-Felipe, A., Ribes-Greus, A., 2012b. Hygrothermal ageing of reprocessed polylactide. Polym. Degrad. Stab. 97 (10), 1881–1890. https://doi.org/10.1016/j.polymdegradstab.2012.06.001. Oct.

Badia, J.D., Santonja-Blasco, L., Martínez-Felipe, A., Ribes-Greus, A., Martínez-Felipe, A., Ribes-Greus, A., 2012c. Reprocessed polylactide: studies of thermo-oxidative decomposition. Bioresour. Technol. 114 (0), 622–628. https://doi.org/10.1016/j.biortech.2012.02.128. Jun.

Badia, J.D., Strömberg, E., Karlsson, S., Ribes-Greus, A., 2012d. Material valorisation of amorphous polylactide. influence of thermo-mechanical degradation on the morphology, segmental dynamics, thermal and mechanical performance. Polym. Degrad. Stab. 97 (4), 670–678. https://doi.org/10.1016/j.polymdegradstab.2011.12.019. Apr.

Badia, J.D., Strömberg, E., Kittikorn, T., Ek, M., Karlsson, S., Ribes-Greus, A., 2017c. Relevant factors for the eco-design of polylactide/sisal biocomposites to control biodegradation in soil in an end-of-life scenario. Polym. Degrad. Stab. 143, 9–19. https://doi.org/10.1016/j.polymdegradstab.2017.06.004. Sep.

Badia, J.D., Strömberg, E., Ribes-Greus, A., Karlsson, S., 2011. Assessing the maldi-tof ms sample preparation procedure to analyze the influence of thermo-oxidative ageing and thermo-mechanical degradation on poly(lactide). Eur. Polym. J. 47 (7), 1416–1428. https://doi.org/10.1016/j.eurpolymj.2011.05.001. Jul.

Brizga, J., Hubacek, K., Feng, K., 2020. The unintended side effects of bioplastics: carbon, land, and water footprints. One Earth. 3 (1), 45–53. https://doi.org/10.1016/J.ONEEAR.2020.06.016. Jul.

C. of the E. U. European Parliament, "Directive (EU) 2019/904 of the European Parliament and of the Council of 5 June 2019 on the reduction of the impact of certain plastic products on the environment," Brussels, 2019.

Chaudhary, A., Srivastava, R., 2023. Ionic liquid-assisted depolymerization of condensation polymers: a review. ChemistrySelect. 8 (30), e202301709 https://doi.org/10.1002/SLCT.202301709. Aug.

S.S. Chavan, Y.O. Sharma, and M.S. Degani, "Cost-effective ionic liquid for environmentally friendly synthesis of 3,4-dihydropyrimidin-2(1H)-ones," *http://mc.manuscriptcentral.com/tgcl*, vol. 2, no. 3, pp. 175–179, 2009, doi: 10.1080/17518250903252260.

Choi, H.-M., Kwon, I., 2011. Dissolution of zein using protic ionic liquids: *n* -(2-hydroxyethyl) ammonium formate and *n* -(2-hydroxyethyl) ammonium acetate. Ind. Eng. Chem. Res. 50 (4), 2452–2454. https://doi.org/10.1021/ie1007745. Feb.

Codari, F., Lazzari, S., Soos, M., Storti, G., Morbidelli, M., Moscatelli, D., 2012. Kinetics of the hydrolytic degradation of poly(lactic acid). Polym. Degrad. Stab. 97 (11), 2460–2466. https://doi.org/10.1016/J.POLYMDEGRADSTAB.2012.06.026. Nov.

Cosate de Andrade, M.F., Souza, P.M.S., Cavalett, O., Morales, A.R., 2016. Life cycle assessment of poly(lactic acid) (PLA): comparison between chemical recycling, mechanical recycling and composting. J. Polym. Environ. 24 (4), 372–384. https://doi.org/10.1007/s10924-016-0787-2. Dec.

Cristina, A.M., Sara, F., Fausto, G., Vincenzo, P., Rocchina, S., Claudio, V., 2018. Degradation of post-consumer PLA: hydrolysis of polymeric matrix and oligomers stabilization in aqueous phase. J. Polym. Environ. 26 (12), 4396–4404. https://doi.org/10.1007/s10924-018-1312-6. Dec.

Cui, Y., et al., 2016. Experimental and theoretical studies on compositions, structures, and IR and NMR spectra of functionalized protic ionic liquids. Phys. Chem. Chem. Phys. 18 (29), 19731–19737. https://doi.org/10.1039/C6CP03293A. Jul.

De Maere D'aertrycke, J.B., Morlot, J., Robeyns, K., Filinchuk, Y., Leyssens, T., 2020. Exploring the solid-state phases and thermodynamics of calcium L-lactate. Food Chem. 325, 126884 https://doi.org/10.1016/J.FOODCHEM.2020.126884. Sep.

E. Commission et al., "A circular economy for plastics: insights from research and innovation to inform policy and funding decisions," Publications Office, 2019. doi: 10.2777/269031.

Elsawy, M.A., Kim, K.H., Park, J.W., Deep, A., 2017. Hydrolytic degradation of polylactic acid (PLA) and its composites. Renew. Sustain. Energy Rev. 79, 1346–1352. https://doi.org/10.1016/J.RSER.2017.05.143. Nov.

European Bioplastics, "Bioplastics Market Development Update 2022," Berlin, 2022. Accessed: Sep. 19, 2023. [Online]. Available: https://docs.european-bioplastics.org/publications/market_data/2022/Report_Bioplastics_Market_Data_2022_short_version.pdf.

European Bioplastics, "EU Policy Framework on Biobased, Biodegradable and Compostable Plastics," Berlin, 2023. Accessed: Sep. 19, 2023. [Online]. Available: https://docs.european-bioplastics.org/publications/pp/EUBP_Statement_Policy_framework_biobased_biodegradable_and_compostable_plastics.pdf.

Ghahramani, S., Yousefi, F., Hosseini, S.M., Aparicio, S., 2020. High-pressure behavior of 2-hydroxyethylammonium acetate ionic liquid: experiment and molecular dynamics. J. Supercrit. Fluids. 155, 104664 https://doi.org/10.1016/J.SUPFLU.2019.104664. Jan.

Ghandi, K., 2014. A review of ionic liquids, their limits and applications. Green Sustain. Chem. 04 (01), 44–53. https://doi.org/10.4236/GSC.2014.41008.

Gil-Castell, O., et al., 2014. Hydrothermal ageing of polylactide/sisal biocomposites. Studies of water absorption behaviour and Physico-Chemical performance. Polym. Degrad. Stab. 108, 212–222. https://doi.org/10.1016/j.polymdegradstab.2014.06.010. Oct.

Gil-Castell, O., et al., 2016. Impact of hydrothermal ageing on the thermal stability, morphology and viscoelastic performance of PLA/sisal biocomposites. Polym. Degrad. Stab. 132, 87–96. https://doi.org/10.1016/j.polymdegradstab.2016.03.038. Mar.

Gil-Castell, O., Andres-Puche, R., Dominguez, E., Verdejo, E., Monreal, L., Ribes-Greus, A., 2020. Influence of substrate and temperature on the biodegradation of polyester-based materials: polylactide and poly(3-hydroxybutyrate-co-3-hydroxyhexanoate) as model cases. Polym. Degrad. Stab. 180, 109288 https://doi.org/10.1016/j.polymdegradstab.2020.109288. Oct.

Gil-Castell, O., Badia, J.D., Ingles-Mascaros, S., Teruel-Juanes, R., Serra, A., Ribes-Greus, A., 2018a. Polylactide-based self-reinforced composites biodegradation: individual and combined influence of temperature, water and compost. Polym. Degrad. Stab. 158, 40–51. https://doi.org/10.1016/j.polymdegradstab.2018.10.017. Dec.

Gil-Castell, O., Badia, J.D., Ribes-Greus, A., 2018b. Suitability of blends from virgin and reprocessed polylactide: performance and energy valorization kinetics. J. Renew. Mater. 6 (4), 370–382. https://doi.org/10.7569/JRM.2017.634170.

Gil-Castell, O., Wolf, M.H., Cea, J., Carrasco, J.C., Giacinti Baschetti, M., Ribes-Greus, A., 2022. Structure–properties relationship of reprocessed bionanocomposites of plasticized polylactide reinforced with nanofibrillated cellulose. Appl. Sci. (Switzerland) 12 (24), 12821. https://doi.org/10.3390/APP122412821/S1. Dec.

Gironi, F., Frattari, S., Piemonte, V., 2016. PLA chemical recycling process optimization: pla solubilization in organic solvents. J. Polym. Environ. 24 (4), 328–333. https://doi.org/10.1007/s10924-016-0777-4. Dec.

Greaves, T.L., Drummond, C.J., 2008. Protic ionic liquids: properties and applications. Chem. Rev. 108 (1), 206–237. https://doi.org/10.1021/cr068040u. Jan.

Hakkarainen, M., Finne-Wistrand, A., 2011. Polylactide. In: Handbook of Engineering and Speciality Thermoplastics: Polyethers and Polyesters, 3, pp. 349–376. https://doi.org/10.1002/9781118104729.CH9. Jun.

Horodytska, O., Cabanes, A., Fullana, A., 2020. Non-intentionally added substances (NIAS) in recycled plastics. Chemosphere 251, 126373. https://doi.org/10.1016/J.CHEMOSPHERE.2020.126373. Jul.

Hosseini, S.M., Hosseinian, A., Aparicio, S., 2019. An experimental and theoretical study on 2-hydroxyethylammonium acetate ionic liquid. J. Mol. Liq. 284, 271–281. https://doi.org/10.1016/J.MOLLIQ.2019.03.150. Jun.

Jiang, B., et al., 2015. Synthesis of chlorostannate(II) ionic liquids and their novel application in the preparation of high-quality L-lactide. RSC. Adv. 5 (63), 50747–50755. https://doi.org/10.1039/C5RA05073A. Jun.

Kang, L.-Q., Cao, Z.-J., Lei, Z.-J., 2016. 2-Hydroxyethylammonium acetate: an efficient and reusable homogeneous catalyst for the synthesis of Hantzsch 1,4-dihydropyridines. Monatsh. Chem. - Chemical Monthly 147 (6), 1125–1128. https://doi.org/10.1007/s00706-015-1587-4. Jun.

Kiran-Yildirim, B., Titiz-Sargut, S., Sayan, P., 2018. Calcium lactate pentahydrate crystallization in the presence of pentanoic acid. Chem. Eng. Technol. 41 (6), 1244–1251. https://doi.org/10.1002/CEAT.201700672. Jun.

Koutsoukos, S., et al., 2022. Synthesis of aprotic ionic liquids. Nat. Rev. Methods Primers 2 (1), 1–18. https://doi.org/10.1038/s43586-022-00129-3. *2022 2:1*Jun.

Kurnia, K.A., Harris, F., Wilfred, C.D., Abdul Mutalib, M.I., Murugesan, T., 2009. Thermodynamic properties of CO2 absorption in hydroxyl ammonium ionic liquids at pressures of (100–1600) kPa. J Chem Thermodyn 41 (10), 1069–1073. https://doi.org/10.1016/J.JCT.2009.04.003. Oct.

Lamberti, F.M., Román-Ramírez, L.A., Wood, J., 2020. Recycling of bioplastics: routes and benefits. J. Polym. Environ. 28 (10), 2551–2571. https://doi.org/10.1007/S10924-020-01795-8. *2020 28:10*Jun.

Li, M., Zhang, S., 2024a. Tandem chemical depolymerization and photoreforming of waste pet plastic to high-value-added chemicals. ACS. Catal. 14 (5), 2949–2958. https://doi.org/10.1021/acscatal.3c05535. Mar.

Li, M., Zhang, S., 2024b. Coupling waste plastic upgrading and co $_2$ photoreduction to high-value chemicals by a binuclear *re*–ru heterogeneous catalyst. ACS. Catal. 14 (9), 6717–6727. https://doi.org/10.1021/acscatal.4c00444. May.

Li, X.G., Lv, Y., Ma, B.G., Wang, W.Q., Jian, S.W., 2017. Decomposition kinetic characteristics of calcium carbonate containing organic acids by TGA. Arab. J. Chem. 10, S2534–S2538. https://doi.org/10.1016/J.ARABJC.2013.09.026. May.

Liu, H., et al., 2017. Lewis acidic ionic liquid [Bmim]FeCl4 as a high efficient catalyst for methanolysis of poly (lactic acid). Catal. Letters. 147 (9), 2298–2305. https://doi.org/10.1007/s10562-017-2138-x. Sep.

Liu, H., Song, X., Liu, F., Liu, S., Yu, S., 2015. Ferric chloride as an efficient and reusable catalyst for methanolysis of poly(lactic acid) waste. J. Polym. Res. 22 (7) https://doi.org/10.1007/s10965-015-0783-6.

Majgaonkar, P., Hanich, R., Malz, F., Brüll, R., 2021. Chemical Recycling of Post-Consumer PLA Waste for Sustainable Production of Ethyl Lactate. Chemical Engineering Journal 423, 129952. https://doi.org/10.1016/J.CEJ.2021.129952. Nov.

McKeown, P., Jones, M.D., 2020. The Chemical Recycling of PLA: a Review. Sustain. Chem. 1 (1), 1–22. https://doi.org/10.3390/SUSCHEM1010001. *2020*vol. 11–22May.

Mohd-Adnan, A.-F.F., Nishida, H., Shirai, Y., 2008. Evaluation of kinetics parameters for poly(l-lactic acid) hydrolysis under high-pressure steam. Polym. Degrad. Stab. 93 (6), 1053–1058. https://doi.org/10.1016/j.polymdegradstab.2008.03.022. Jun.

Moliner, C., et al., 2017. Mechanical and thermal performance of PLA and PHBV-based biopolymers as potential alternatives to PET. Chem. Eng. Trans. 57, 1417–1422. https://doi.org/10.3303/CET1757237. *57*.

Moliner, C., et al., 2018. Thermal kinetics for the energy valorisation of polylactide/sisal biocomposites. Thermochim. Acta 670, 169–177. https://doi.org/10.1016/j.tca.2018.10.029.

Mukerjee, R., Wu, C.F.J., 2006. A Modern Theory of Factorial Designs, 1st ed. Springer New York, New York, NY. https://doi.org/10.1007/0-387-37344-6.

Oliveira, M.V.S., et al., 2016. (Eco)toxicity and biodegradability of protic ionic liquids. Chemosphere 147, 460–466. https://doi.org/10.1016/J.CHEMOSPHERE.2015.11.016. Mar.

Paiva, R., Pereira-Filho, E.R., Wrona, M., Cruz, S.A., 2024. Optimization of washing parameters to minimize the degradation of poly(lactic acid) using design of experiments: a contribution to the recycling chain. J. Polym. Environ. 32 (4), 1650–1657. https://doi.org/10.1007/s10924-023-03075-7. Apr.

Pang, X., Zhuang, X., Tang, Z., Chen, X., 2010. Polylactic acid (PLA): research, development and industrialization. Biotechnol. J. 5 (11), 1125–1136. https://doi.org/10.1002/BIOT.201000135. Nov.

Pascual-Jose, B., Badia, J.D., Múgica, A., Addiego, F., Müller, A.J., Ribes-Greus, A., 2021. Analysis of plasticization and reprocessing effects on the segmental cooperativity of polylactide by dielectric thermal spectroscopy. Polymer. (Guildf) 223, 123701. https://doi.org/10.1016/J.POLYMER.2021.123701. May.

Payne, J., Jones, M.D., 2021. The chemical recycling of polyesters for a circular plastics economy: challenges and emerging opportunities. ChemSusChem. 14 (19), 4041–4070. https://doi.org/10.1002/CSSC.202100400. Oct.

Pellis, A., Malinconico, M., Guarneri, A., Gardossi, L., 2021. Renewable polymers and plastics: performance beyond the green. N. Biotechnol. 60, 146–158. https://doi.org/10.1016/J.NBT.2020.10.003. Jan.

Pérez-Fonseca, A.A., González-López, M.E., Robledo-Ortíz, J.R., 2023. Reprocessing and recycling of poly(Lactic Acid): a review. J. Polym. Environ. 31 (10), 4143–4159. https://doi.org/10.1007/s10924-023-02919-6. Oct.

Petrus, R., Bykowski, D., Sobota, P., 2016. Solvothermal alcoholysis routes for recycling polylactide waste as lactic acid esters. ACS. Catal. 6 (8), 5222–5235. https://doi.org/10.1021/acscatal.6b01009. Aug.

Piemonte, V., Gironi, F., 2013a. Lactic acid production by hydrolysis of poly(Lactic Acid) in aqueous solutions: an experimental and kinetic study. J. Polym. Environ. 21 (1), 275–279. https://doi.org/10.1007/s10924-012-0468-8. Mar.

Piemonte, V., Gironi, F., 2013b. Kinetics of hydrolytic degradation of PLA. J. Polym. Environ. 21 (2), 313–318. https://doi.org/10.1007/s10924-012-0547-x. Jun.

Piemonte, V., Sabatini, S., Gironi, F., 2013. Chemical recycling of PLA: a great opportunity towards the sustainable development? J. Polym. Environ. 21 (3), 640–647. https://doi.org/10.1007/s10924-013-0608-9.

Plastics Europe, "Plastics – the Facts 2022." [Online]. Available: https://plasticseurope.org/knowledge-hub/plastics-the-facts-2022/.

Polat, S., 2022. Thermal degradation of calcium lactate pentahydrate using TGA/FTIR/MS: thermal kinetic and thermodynamics studies. Indian Chem. Eng. 64 (4), 402–415. https://doi.org/10.1080/00194506.2021.2017359. Aug.

RameshKumar, S., Shaiju, P., O'Connor, K.E., P, R.B., 2020. Bio-based and biodegradable polymers - State-of-the-art, challenges and emerging trends. Curr. Opin. Green. Sustain. Chem. 21, 75–81. https://doi.org/10.1016/J.COGSC.2019.12.005. Feb.

Reid, J.E.S.J., Prydderch, H., Spulak, M., Shimizu, S., Walker, A.J., Gathergood, N., 2018. Green profiling of aprotic versus protic ionic liquids: synthesis and microbial toxicity of analogous structures. Sustain. Chem. Pharm. 7, 17–26. https://doi.org/10.1016/J.SCP.2017.11.001. Mar.

Rocha, E.G.A., Pin, T.C., Rabelo, S.C., Costa, A.C., 2017. Evaluation of the use of protic ionic liquids on biomass fractionation. Fuel 206, 145–154. https://doi.org/10.1016/J.FUEL.2017.06.014. Oct.

Román-Ramírez, L.A., Mckeown, P., Jones, M.D., Wood, J., 2019. Poly(lactic acid) degradation into methyl lactate catalyzed by a well-defined Zn(II) complex. ACS. Catal. 9 (1), 409–416. https://doi.org/10.1021/acscatal.8b04863. Jan.

Román-Ramírez, L.A., McKeown, P., Shah, C., Abraham, J., Jones, M.D., Wood, J., 2020. Chemical degradation of end-of-life poly(lactic acid) into methyl lactate by a Zn(II) complex. Ind. Eng. Chem. Res. 59 (24), 11149–11156. https://doi.org/10.1021/acs.iecr.0c01122. Jun.

S.-G. European Commission, "A European Strategy for Plastics in a Circular Economy," Brussels, 2018. Accessed: Sep. 19, 2023. [Online]. Available: https://eur-lex.europa.eu/legal-content/EN/TXT/?qid=1516265440535&uri=COM:2018:28:FIN.

Sakata, Y., Shiraishi, S., Otsuka, M., 2005. Characterization of dehydration and hydration behavior of calcium lactate pentahydrate and its anhydrate. Colloids. Surf. B Biointerfaces. 46 (3), 135–141. https://doi.org/10.1016/J.COLSURFB.2005.10.004. Dec.

Seesanong, S., et al., 2022. Economical and environmentally friendly track of biowaste recycling of scallop shells to calcium lactate. ACS. Omega 7 (17), 14756–14764. https://doi.org/10.1021/acsomega.2c00112. May.

Sepúlveda, F.A., et al., 2022. Poly (lactic acid)/D-limonene/ZnO bio-nanocomposites with antimicrobial properties. J. Appl. Polym. Sci. 139 (4), 51542. https://doi.org/10.1002/APP.51542. Jan.

Siddiqui, M.N., Kolokotsiou, L., Vouvoudi, E., Redhwi, H.H., Al-Arfaj, A.A., Achilias, D. S., 2020. Depolymerization of PLA by phase transfer catalysed alkaline hydrolysis in a microwave reactor. J. Polym. Environ. 28 (6), 1664–1672. https://doi.org/10.1007/S10924-020-01716-9/SCHEMES/2. Jun.

Sin, L.T., Rahmat, A.R., Rahman, W.A.W.A., 2013. Thermal properties of poly(lactic Acid). Polylactic Acid 109–141. https://doi.org/10.1016/B978-1-4377-4459-0.00003-2. Jan.

Sobhani, S., Honarmand, M., 2013. 2-Hydroxyethylammonium acetate: a reusable task-specific ionic liquid promoting one-pot, three-component synthesis of 2-amino-3,5-dicarbonitrile-6-thio-pyridines. Comptes Rendus Chimie 16 (3), 279–286. https://doi.org/10.1016/J.CRCI.2012.10.011. Mar.

Solis, M., Silveira, S., 2020. Technologies for chemical recycling of household plastics – A technical review and TRL assessment. Waste Management 105, 128–138. https://doi.org/10.1016/J.WASMAN.2020.01.038. Mar.

Song, X., Bian, Z., Hui, Y., Wang, H., Liu, F., Yu, S., 2019. Zn-Acetate-Containing ionic liquid as highly active catalyst for fast and mild methanolysis of Poly(lactic acid). Polym. Degrad. Stab. 168, 108937 https://doi.org/10.1016/J.POLYMDEGRADSTAB.2019.108937. Oct.

Song, X., Wang, H., Yang, X., Liu, F., Yu, S., Liu, S., 2014a. Hydrolysis of poly(lactic acid) into calcium lactate using ionic liquid [Bmim][OAc] for chemical recycling. Polym. Degrad. Stab. 110, 65–70. https://doi.org/10.1016/J.POLYMDEGRADSTAB.2014.08.020. Dec.

Song, X., Wang, H., Zheng, X., Liu, F., Yu, S., 2014b. Methanolysis of poly(lactic acid) using acidic functionalized ionic liquids as catalysts. J. Appl. Polym. Sci. 131 (19), 40817. https://doi.org/10.1002/APP.40817. Oct.

Song, X., Zhang, X., Wang, H., Liu, F., Yu, S., Liu, S., 2013. Methanolysis of poly(lactic acid) (PLA) catalyzed by ionic liquids. Polym. Degrad. Stab. 98 (12), 2760–2764. https://doi.org/10.1016/J.POLYMDEGRADSTAB.2013.10.012. Dec.

Speranza, V., De Meo, A., Pantani, R., 2014. Thermal and hydrolytic degradation kinetics of PLA in the molten state. Polym. Degrad. Stab. 100 (1), 37–41. https://doi.org/10.1016/J.POLYMDEGRADSTAB.2013.12.031. Feb.

Tsuji, H., Daimon, H., Fujie, K., 2003. A new strategy for recycling and preparation of poly(l-lactic acid): hydrolysis in the melt. Biomacromolecules. 4 (3), 835–840. https://doi.org/10.1021/bm034060j. May.

Tsuneizumi, Y., Kuwahara, M., Okamoto, K., Matsumura, S., 2010. Chemical recycling of poly(lactic acid)-based polymer blends using environmentally benign catalysts. Polym. Degrad. Stab. 95 (8), 1387–1393. https://doi.org/10.1016/j.polymdegradstab.2010.01.019. Aug.

United Nations (UN), "Sustainable development goals (SDGs)." Accessed: Nov. 29, 2022. [Online]. Available: https://sdgs.un.org/goals.

Wolf, M.H., Gil-Castell, O., Cea, J., Carrasco, J.C., Ribes-Greus, A., 2023. Degradation of plasticised Poly(lactide) composites with nanofibrillated cellulose in different

hydrothermal environments. J. Polym. Environ. 31 (5), 2055–2072. https://doi.org/10.1007/s10924-022-02711-y. May.
Yang, R., Xu, G., Dong, B., Hou, H., Wang, Q., 2022. A 'Polymer to Polymer' Chemical Recycling of PLA Plastics by the 'DE–RE Polymerization' Strategy. Macromolecules. 55 (5), 1726–1735. https://doi.org/10.1021/acs.macromol.1c02085. Mar.
Ye, Y.S., Rick, J., Hwang, B.J., 2013. Ionic liquid polymer electrolytes. J. Mater. Chem. a Mater. 1 (8), 2719–2743. https://doi.org/10.1039/C2TA00126H. Jan.
Yuan, X.L., Zhang, S.J., Lu, X.M., 2007. Hydroxyl ammonium ionic liquids: synthesis, properties, and solubility of SO $_2$. J. Chem. Eng. Data 52 (2), 596–599. https://doi.org/10.1021/je060479w. Mar.
Zhang, L., Fu, X., Gao, G., 2011. Anion–cation cooperative catalysis by ionic liquids. ChemCatChem. 3 (8), 1359–1364. https://doi.org/10.1002/CCTC.201100016. Aug.
Zhang, S., et al., 2023a. Depolymerization of polyesters by a binuclear catalyst for plastic recycling. Nat. Sustain. 2023 6 (8), 965–973. https://doi.org/10.1038/s41893-023-01118-4. *6:8*May.
Zhang, S., Li, M., Zuo, Z., Niu, Z., 2023b. Recent advances in plastic recycling and upgrading under mild conditions. Green Chem. 25 (18), 6949–6970. https://doi.org/10.1039/D3GC01872E. Sep.
Zhang, S., Xue, Y., Wu, Y., Zhang, Y.X., Tan, T., Niu, Z., 2023c. PET recycling under mild conditions via substituent-modulated intramolecular hydrolysis. Chem. Sci. 14 (24), 6558–6563. https://doi.org/10.1039/D3SC01161E. Jun.
Zimmermann, L., Dierkes, G., Ternes, T.A., Völker, C., Wagner, M., 2019. Benchmarking the in vitro toxicity and chemical composition of plastic consumer products. Environ. Sci. Technol. 53 (19), 11467–11477. https://doi.org/10.1021/acs.est.9b02293. Oct.